

A Model for the Spectral Albedo of Snow. II: Snow Containing Atmospheric Aerosols

STEPHEN G. WARREN¹ AND WARREN J. WISCOMBE

National Center for Atmospheric Research,² Boulder, CO 80307

(Manuscript received 15 April 1980, in final form 28 August 1980)

ABSTRACT

Small highly absorbing particles, present in concentrations of only 1 part per million by weight (ppmw) or less, can lower snow albedo in the visible by 5–15% from the high values (96–99%) predicted for pure snow in Part I. These particles have, however, no effect on snow albedo beyond 0.9 μm wavelength where ice itself becomes a strong absorber. Thus we have an attractive explanation for the discrepancy between theory and observation described in Part I, a discrepancy which seemingly cannot be resolved on the basis of near-field scattering and nonsphericity effects.

Desert dust and carbon soot are the most likely contaminants. But careful measurements of spectral snow albedo in the Arctic and Antarctic point to a “grey” absorber, one whose imaginary refractive index is nearly constant across the visible spectrum. Thus carbon soot, rather than the red iron oxide normally present in desert dust, is strongly indicated at these sites. Soot particles of radius 0.1 μm , in concentrations of only 0.3 ppmw, can explain the albedo measurements of Grenfell and Maykut on Arctic Ice Island T-3. This amount is consistent with some observations of soot in Arctic air masses. 1.5 ppmw of soot is required to explain the Antarctic observations of Kuhn and Siogas, which seemed an unrealistically large amount for the earth’s most unpolluted continent until we learned that burning of camp heating fuel and aircraft exhaust indeed had contaminated the measurement site with soot.

Midlatitude snowfields are likely to contain larger absolute amounts of soot and dust than their polar counterparts, but the snowfall is also much larger, so that the ppmw contamination does not differ drastically until melting begins. Nevertheless, the variations in absorbing particle concentration which *will* exist can help to explain the wide range of visible snow albedos reported in the literature.

Longwave emissivity of snow is unaltered by its soot and dust content. Thus the depression of snow albedo in the visible is a systematic effect and always results in more energy being absorbed at a snow-covered surface than would be the case for pure snow. Thus man-made carbon soot aerosol may continue to exert a significant warming effect on the earth’s climate even after it is removed from the atmosphere.

1. Introduction

In Part I of this paper (Wiscombe and Warren, 1980) a model for calculating snow spectral albedo was presented. The comparison of its results with observations showed good agreement in the near-infrared (near-IR), where the reduction in snow albedo with age could be mimicked by reasonable increases in snow grain size (Part I, Figs. 10 and 15). For the visible wavelengths, however, where the albedo is highest, the model consistently calculated albedos higher than are normally observed. The discrepancy is greater for melting snow than for new snow.

Fig. 1 illustrates the problem we are confronting. The solid line is a recent measurement of spectral albedo at South Pole Station by Kuhn and Siogas (1978). In order for our model predictions (the small

circles) to match these observations in the near-IR ($0.9 \leq \lambda \leq 1.5 \mu\text{m}$) we require a snow grain radius $r = 100 \mu\text{m}$, which is reasonable for the surface of the Antarctic plateau (Stephenson, 1967). But using this grain radius at shorter wavelengths results in albedos up to 10% higher than observed. A larger grain size would reduce the albedo at *all* wavelengths, thus destroying our good agreement in the near-IR.

The probable presence of absorbing impurities in the snow provides a way out of this dilemma. Because ice is so weakly absorptive in the visible region, very small amounts of dust or soot may be capable of reducing the albedo there, while having little effect in the near-IR where ice itself is highly absorptive. Our hypothesis, then, is that measured snow albedos at visible wavelengths are significantly lower than pure-snow values due to the presence of dust or soot.

Using the simple model of Part I, we show below how snow albedo depends on dust concentration, dust composition and dust particle sizes. We investigate first the effect of desert dust, which is a

¹ Present affiliation: Cooperative Institute for Research in Environmental Sciences, University of Colorado, Boulder 80309.

² The National Center for Atmospheric Research is sponsored by the National Science Foundation.

mixture of materials whose aggregate optical properties have been studied, and second the effect of carbon soot alone, which may normally be the principal absorptive component of atmospheric aerosols that find their way into snow.

2. Observations relating to atmospheric aerosols in snow

Dust enters snow as ice nuclei, as particles scavenged by falling snow crystals, and by fallout. Clay mineral particles, blown up primarily from the world's deserts, form a major component of the global background aerosol (Pruppacher and Klett, 1978). These dust particles can travel thousands of kilometers to reach snow-covered regions (Prospero, 1979, and references therein).

Snow crystals are usually nucleated by micron-sized clay mineral particles, and the crystals become effective scavengers when they fall. Magono *et al.* (1979) found falling snow crystals to have collection efficiency near unity for all aerosols in the size range 0.1 to 5.0 μm . The third mechanism—fallout—is also important, at least in midlatitudes. Falconer and Hogan (1971) found much more dust in snow on the ground than they found in falling snowflakes.

The dust incorporated into snow by all three mechanisms is predominantly clay minerals, except where the marine influence is strong, e.g., over Antarctica, where sea salts tend to dominate. But we can ignore sea salts in this study because they are almost perfectly transparent at solar wavelengths (Toon *et al.*, 1976). Many of the clay minerals are also relatively transparent, but they typically have highly absorptive inclusions such as iron oxide, carbon or organic materials (Lindberg, 1975).

Kumai (1976, 1977) has identified the impurities in falling snow at Camp Century (Greenland) and at the South Pole. He typically found one large nucleus at the center and several smaller particles (presumably scavenged) elsewhere in each snow crystal. At Camp Century 84% of the nuclei were clay minerals, 10% unidentified insoluble minerals and 1% soluble sea salt (5% had no nucleus). Kumai found the bulk concentration of clay mineral particles in falling snow to be 0.034 ppmw, and most of these particles were at the centers of snow crystals. This compares with the value of 0.035 ppmw found earlier by Murozumi *et al.* (1969) and with a value of 0.050 ppmw we calculate from data of Hamilton and Langway (1967). Kumai found a size distribution somewhat resembling a Junge power law, but with a plateau around 1 μm , which is the typical average size of these particles.

At the South Pole, Kumai found considerably more soluble particles in the snow (20%) but still the

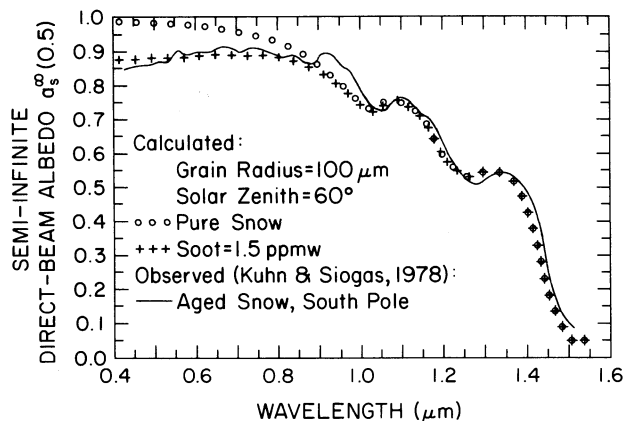


FIG. 1. Snow albedo at South Pole Station, calculation and measurement.

majority (59%) of the nuclei were clay minerals. The total clay mineral concentration was lower than in Greenland, only 0.015 ppmw. Murozumi *et al.* (1969) obtained an even lower estimate, only 0.002 ppmw of terrestrial dust, at Byrd Station (West Antarctica) by multiplying the silicon concentration by 5.

This enhancement of sea salt relative to continental dust, and the very low total concentrations of continental dust in Antarctic aerosol, can be attributed to the long distance from significant sources of dust in Australia and southern Africa. The frequent storms in the oceanic zone surrounding Antarctica remove much dust by rainout and washout, making Antarctic snow the cleanest on earth.

These dust concentrations in falling snow are usually preserved if there is no melting. Dust is found in all polar ice cores (Thompson, 1977; Hammer, 1977; Koerner, 1977). Dust has been used to identify annual layers even at locations where snowmelt does not occur, because a maximum is found every spring at some locations (Langway *et al.*, 1977; Hammer, 1977).

Dust layers are found in temperate glaciers (Post and LaChapelle, 1971, Figs. 6–11) corresponding to the summer melt season. This may be due to clay-mineral dust accumulating at the surface instead of percolating down with the meltwater, or to dry fallout during the time of no snowfall (Kohn and Maeno, 1979). Dust concentrations measured in these dirty layers presumably are representative of the end of the melt season. For example, Koerner (1977, Fig. 3) shows concentrations of dust in the annual dirty layers of an ice core on Devon Island to be 5–10 times as high as concentrations in the intervening clean layers. The top of Devon Island undergoes a short melt season (July only), so the concentrating of dust would presumably be larger where the melt season is longer.

At lower latitudes we might expect considerably

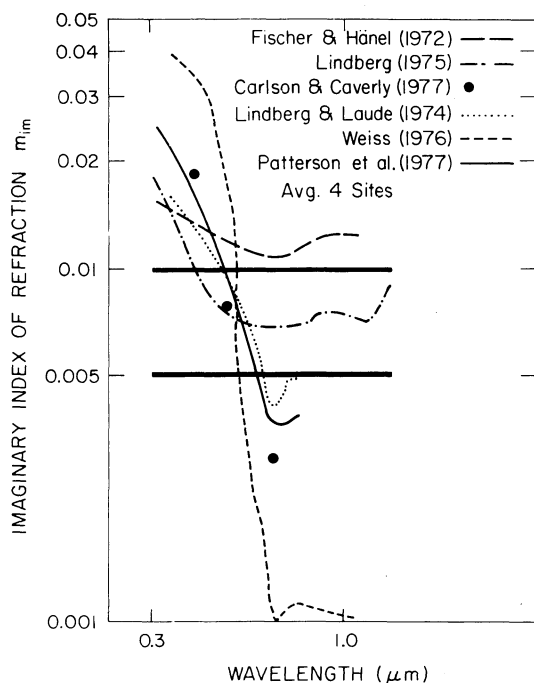


FIG. 2. Imaginary index of refraction for desert dust as a function of wavelength from various sources; taken from Carlson and Benjamin (1980, Fig. 3).

higher dust concentrations than those cited above. Dust concentrations in the surface layer of a perennial mountain snowfield in Japan during the melt season were reported by Higuchi and Nagoshi (1977), who simultaneously measured total albedo. The average dust concentration between 30 and 300 cm below the surface was 5 ppmw at the beginning of the melt season; i.e., this "clean" snow already contained 100 times the dust concentration found on the Greenland and Antarctic plateaus. As the summer progressed, the particulate matter was found to be retained in the topmost 1 cm. The dust concentration in this topmost centimeter at the beginning of the melt season (June) was already 100 ppm. The spectrally-integrated albedo was observed to drop from 60% (for 100 ppm dust) to 15% (for 4000 ppm dust).

For the Quelccaya Ice Cap at 14°S in the Andes (Thompson *et al.*, 1979), the average dust concentration was 5 ppm for snow 4.5–5.5 m below the surface. The dirtiest sample contained 8.8 ppmw dust, whereas the cleanest contained 1.2 ppmw. These concentrations are two orders of magnitude greater than those found in Antarctic snow, but close to those found by Higuchi and Nagoshi (1977) in Japan. The dust particle size distribution for Quelccaya has an effective mean radius (for snow albedo purposes) of about $r = 1.3 \mu\text{m}$.

Optical properties of desert dust have been reviewed by Lindberg (1975) and by Carlson and Ben-

jamin (1980). We reproduce Carlson and Benjamin's compilation of the imaginary refractive index in Fig. 2. The measurements of Lindberg and his co-workers were for desert dust collected in southern New Mexico. Most of the others were for dust which blew off the Sahara over the North Atlantic. There are considerable differences among the various investigations. Patterson *et al.* (1977) reported good agreement for m_{im} among samples collected at four locations spaced across the Atlantic in 1974. Their results show a strong decrease of m_{im} between 0.3 and 0.7 μm wavelength (which would make the dust appear red), but others (in particular Fischer and Hänel, 1972) show m_{im} more nearly constant with wavelength. In the remainder of this paper we use the term "red dust" to refer to dust whose $m_{im}(\lambda)$ is that reported by Patterson *et al.* (1977).

The measured values of m_{im} in the visible region are of the order of 10^{-2} . These values are not characteristic of any pure substance commonly found in soil. Clay minerals have $m_{im} \leq 10^{-4}$ (Lindberg, 1975), while highly absorptive substances like Fe_3O_4 (Becquerel and Rossignol, 1929) or graphitic carbon (Twitty and Weinman, 1971) have $m_{im} \approx 1$; only some volcanic minerals have $10^{-4} < m_{im} < 10^{-1}$ (Pollack *et al.*, 1973). Microscopic investigations indicate that the small highly-absorptive particles stick on to the large clay particles to create a sort of raisin-pudding effect (Lindberg, 1975). Thus the measurements of m_{im} for continental dust represent some sort of average.

The differences in Fig. 2 are probably attributable to variability in dust composition. An abundance of iron oxide would explain the "red dust" curves. The wavelength dependence of m_{im} becomes less steep if the dust contains a grey absorber like graphitic carbon. Lindberg (1975) attempted to match the optical properties of natural New Mexico dust by preparing a synthetic mixture of clay minerals. The synthetic mixture had higher diffuse reflectance at all wavelengths out to 2.5 μm , and steeper wavelength dependence in the visible, than did the natural dust. But, by adding 0.5% by weight of carbon soot to the synthetic mixture, Lindberg was able to match the natural dust reflectance. This suggests that variable soot content may be responsible for many of the differences between measurements in Fig. 2.

Rosen *et al.* (1978) have used Raman spectroscopy to identify the absorbing component in urban aerosols as graphitic carbon. It also has been shown to be the dominant absorber in aerosols collected in rural regions of the United States (Weiss *et al.*, 1979). Graphitic carbon aerosol particles are produced by incomplete combustion in forest fires, brush fires, and industrial furnaces and engines. Seiler and Crutzen (1980) estimate that both natural and industrial sources are of comparable magnitude at present.

Graphitic carbon soot consists of randomly oriented graphite crystallites ($r \approx 20 \text{ \AA}$) embedded in a matrix of amorphous carbon (Franklin, 1950; 1951). Single crystals of pure graphite are highly birefringent, with both m_{re} and m_{im} depending on crystal orientation (Greenaway *et al.*, 1969), but the random arrangement of these crystals in soot means that soot particles will not exhibit optical anisotropy. Soot is generally not pure carbon. The complex refractive index varies as the C/H ratio varies, with m_{im} generally increasing with increasing carbon content (McCartney *et al.*, 1965; Foster and Howarth, 1968; Dalzell and Sarofim, 1969). Because of this, the measured values of $m_{im}(\lambda)$ show some spread, but they generally agree that m_{im} is independent of λ , to within a factor of 2, for $0.3 \leq \lambda \leq 0.9 \mu\text{m}$. Dalzell and Sarofim (1969, Table 1) found, for both acetylene soot and propane soot, $m \approx 1.6 - 0.5i$, essentially independent of wavelength in the visible spectrum. Twitty and Weinman (1971) reviewed some other measurements of m for carbonaceous materials and chose for their calculation a median value (constant with wavelength) $m = 1.8 - 0.5i$. Since we lack exact knowledge of the source and C/H ratio of the graphitic carbon that may be present in snow, we will use the latter value in our calculations below.

There are observations which indicate the efficacy of small particles in reducing snow albedo. Liljequist (1956) noted that in an area downwind from the hut at Maudheim, where soot particles fell out, snowmelt was dramatically accelerated, while elsewhere the snow remained dry. Hanson (1960) also reported reduced snow albedo due to dust or soot from human habitation at an Antarctic station. Dunne and Price (1975) reported that in Labrador aerosol pollution from a small town drops snow albedo down to 50% or less within a few days after each snowfall.

When dust or soot concentrations are very large, the effect on snow albedo can be seen by the naked eye. Elgmork *et al.* (1973) show a photograph of stratigraphy in winter snow in southern Norway. Distinct grey bands suggest episodic pollution events involving soot. Episodic red or yellow snow has also been reported, in conjunction with dust storms in regions adjacent to deserts. Red dust in Alpine snow comes from the Sahara (reviewed by Haeberli, 1977); in New Zealand snow, from Australia (Marshall and Kidson, 1929); in the Tien Shan, from Central Asian deserts (Khromov, 1931; Glazovskaya, 1954); and in the eastern United States, from the American desert and "dust bowl" (Byers, 1936; Robinson, 1936). (Photosynthetic algae growing in melting snow can also give it a red color, but in the examples cited here it was dust rather than algae that produced the color.)

3. Albedo of snow containing desert dust

We shall assume that desert dust is distributed uniformly through a snowpack as spheres with given radii and of density 2.4 g cm^{-3} . The real index of refraction for clay-mineral dust is ~ 1.55 (Carlson and Benjamin, 1980) and we take it to be constant at this value for all wavelengths.

With these assumptions, there remain three dust parameters which affect snow albedo: concentration, mean size, and spectral imaginary refractive index. Mie calculations are done separately for the dust particles and the ice particles and averaged using the respective cross-sectional areas per unit volume as weight factors. The resulting single-scattering coalbedo ($1 - \bar{\omega}$) is shown in Fig. 3a for a snow grain radius $r_{ice} = 1000 \mu\text{m}$, a dust particle mean radius $r_{dust} = 1 \mu\text{m}$, and a "red dust" imaginary index $m_{im}(\text{dust})$. [For $\lambda > 0.7 \mu\text{m}$, $m_{im}(\text{dust})$ is assumed constant and equal to its value at $\lambda = 0.7 \mu\text{m}$.] The dust raises $(1 - \bar{\omega})$ significantly for $\lambda < 0.9 \mu\text{m}$, where $m_{im}(\text{dust}) \gg m_{im}(\text{ice})$. At longer wavelengths, dust concentrations up to 100 ppmw have almost no effect on $\bar{\omega}$ because ice is more absorptive and it swamps the dust effect by virtue of its much larger volume fraction. This is consistent with the observation by Dirmhirn (1960) that an episode of yellow Saharan dust falling into Alpine snow reduced the visible albedo more than it reduced the spectrally integrated albedo (16 and 10% reduction, respectively).

Fig. 4a shows diffuse snow albedo (a_d^{∞}) versus wavelength for 20 ppmw of red dust embedded in snow with grain radii of 1 mm. For fixed concentration, smaller dust particles are always more effective in lowering the albedo than larger ones. The snow would appear grey for $10 \mu\text{m}$ dust particles, but for particles $\leq 1 \mu\text{m}$ a pronounced albedo peak in the red appears, in agreement with certain observations quoted earlier.

Albedos calculated using Kumai's (1977) size distribution for dust in Greenland snow, even when it was extrapolated to include even larger particles, were barely distinguishable from our $r_{dust} = 1 \mu\text{m}$ results in Fig. 4a. The same is true for the particle size distributions measured in both dirty and clean layers of the tropical Quelccaya Ice Cap (elevation 5650 m).

The mean particle size may be larger at lower elevations and nearer to sources. Higuchi and Nagoshi (1977) found the most frequently occurring radius to be 2–5 μm , depending on season, on a mountain snowfield in Japan. Windom (1969) reported size distributions for various minerals from a variety of midlatitude mountain snowfields. The peaks were near $r = 1 \mu\text{m}$ for St. Elias snowfields (Alaska/Yukon) but larger, up to $r = 10 \mu\text{m}$, for snowfields in New Zealand, Mexico and Mt. Olym-

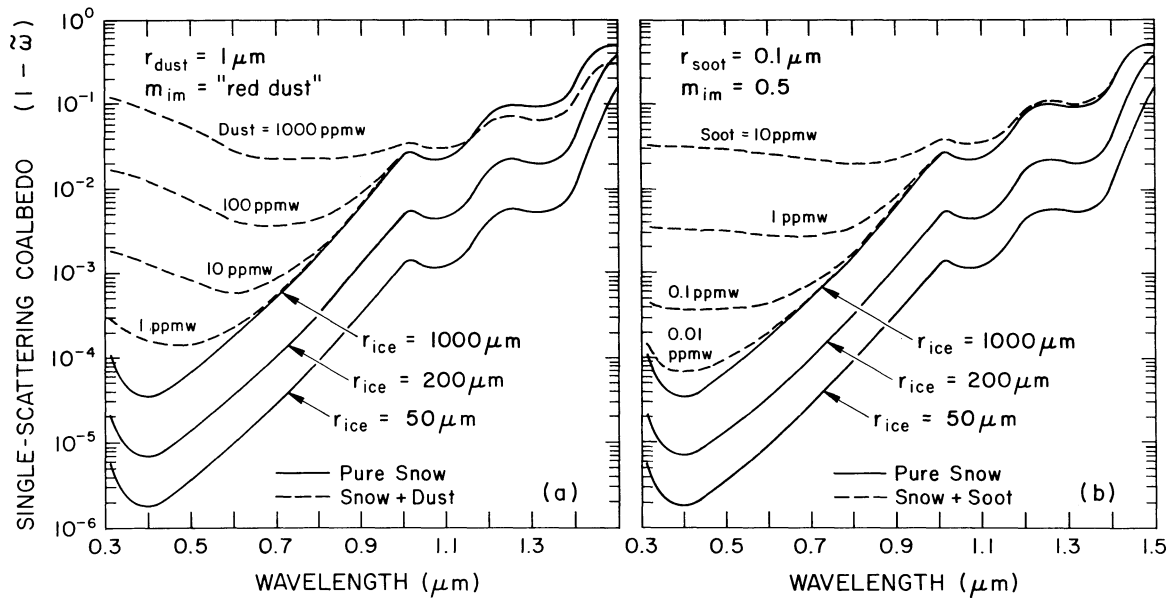


FIG. 3. Effect of solid impurities on single-scattering coalbedo $(1 - \bar{\omega})$. Solid lines are taken from Fig. 3a of Part I. Dashed lines show the effect of adding (a) dust or (b) soot in various concentrations to ice spheres of radius $1000 \mu\text{m}$.

pus (Washington). However, Patterson and Gillette (1977) found the mean radius for soil-derived aerosols to be $1.5 \mu\text{m}$, even at low-elevation continental locations.

Fig. 5 shows albedo calculations for snow containing dust particles of radii $1 \mu\text{m}$ (Figs. 5a and 5c) and $5 \mu\text{m}$ (Figs. 5b and 5d). The incident radiation is a direct beam at solar zenith angle $\theta = 60^\circ$; the results for incident diffuse radiation would be very similar (cf. Part I, Section 5b). We consider $1 \mu\text{m}$ dust particles to be more typical for large snowfields, polar ice caps and snow-covered sea ice, but $5 \mu\text{m}$ particles may be characteristic of snow very near to sources of dust. In each case we have plotted our calculated spectral albedo for pure snow and for snow containing dust in concentrations from 1 to 1000 ppmw. Only albedos for $\lambda < 1.5 \mu\text{m}$ are shown because for longer wavelengths the dust effect is negligible. Note, however, that for very dirty snow (1000 ppmw of dust in Fig. 5c) the albedo for $\lambda > 1 \mu\text{m}$ is substantially increased in the case of fine dust in coarse snow.

For each dust concentration, the albedo in Fig. 5 is plotted using three different spectral imaginary index cases: constant values of 0.005 and 0.01 (the two thick lines in Fig. 2) and the measured values for red dust of Patterson *et al.* (thin solid line in Fig. 2). Calculations using the spectral $m_{\text{im}}(\text{dust})$ of Fischer and Hänel (1972) (shown in Fig. 2) produced results nearly indistinguishable from the case of $m_{\text{im}}(\text{dust}) = 0.01$. The values 0.005 and 0.01 represent reasonable bounds on the measured values of "average imaginary index" (see, e.g., Lindberg, 1975).

The two constant imaginary index cases have essentially similar effects on the snow albedo. They tend to make it a much flatter function of wavelength between 0.3 and $0.8 \mu\text{m}$ than it was without dust, a phenomenon which is similar to the effect of small depth (Fig. 13 of Part I). By contrast, the Patterson imaginary index leads to a very strong wavelength dependence as dust concentration increases, with the visible peak displaced to larger and larger wavelengths. This is especially true for the more realistic case $r_{\text{dust}} = 1 \mu\text{m}$ (Figs. 5a and 5c).

The upper frames in Fig. 5 are for $r_{\text{ice}} = 100 \mu\text{m}$ (new snow); the lower for $r_{\text{ice}} = 1000 \mu\text{m}$ (old melting snow). For the same dust concentration, the albedo is reduced more for $r_{\text{ice}} = 1000 \mu\text{m}$ than for $r_{\text{ice}} = 100 \mu\text{m}$. This is because the radiation penetrates deeper in more coarsely grained snow and encounters more absorbing material before it can re-emerge from the snowpack.

We now attempt to match snow albedo measurements from the central Arctic Ocean by calculating the albedo of snow containing desert dust. In Fig. 6a we take the dust size to be $r = 1 \mu\text{m}$, and its imaginary index that of "red dust." The observations of Grenfell and Maykut (1977) are plotted as solid lines only out to $\lambda = 0.9 \mu\text{m}$, because for $\lambda > 0.9 \mu\text{m}$ the spectral resolution is poor (Grenfell, personal communication). In order of decreasing albedo, the three curves are for dry cold snow, wet new snow, and old melting snow. The snow grain size was chosen in each case as that which produced agreement between calculated and observed albedo at $\lambda = 0.9 \mu\text{m}$ for pure snow, since at this wavelength dust has negligible effect on albedo. The grain sizes were thus

chosen to be $r = 110, 300$ and $1300 \mu\text{m}$, respectively. When these grain sizes are used to calculate albedo for shorter wavelengths, the results for pure snow (circles) exceed the observations.

In order to reduce these calculated values to the observed levels, 10–15 ppmw of dust was required (plus signs in Fig. 6a). The calculated albedo, however, shows a strong spectral variation. If this type of dust were present in snow, the snow would appear red or orange, with a peak in albedo at $\lambda \approx 0.6 \mu\text{m}$. This is clearly not observed for the snow albedo in the central Arctic but may be true for snow in regions closer to deserts. The dotted lines in Fig. 5c show that the wavelength of maximum albedo decreases as the dust concentration is reduced. Thus, the reports of red or yellow snow mentioned above may owe their variability in color to a variability in dust concentration. The dust is normally reported to be red as it falls (Haerberli, 1977), but can appear yellow when diluted in snow. In a firn-core in the high Alps (Oeschger *et al.*, 1977), the snow tentatively assigned to the time of the 1936–37 dustfalls was yellow.

If dust is responsible for the low observed snow albedo at Arctic Ice Island T-3, its m_{im} apparently cannot be that of red dust. If we use the m_{im} obtained for Saharan dust by Fischer and Hänel (1972) or a flat $m_{\text{im}} = 0.005$ independent of wavelength, we obtain rather better agreement with observation. Fig. 6b shows that 13–20 ppm of dust ($m_{\text{im}} = 0.005$) can account for the albedo observations at T-3. However, it is unlikely that this amount of dust is present in Arctic snow. Mullen *et al.* (1972) and Darby *et al.* (1974) reported only 1 ppmw dust in snow at T-3.

4. Albedo of snow containing carbon soot

In order to explain the Grenfell and Maykut albedo measurements, we apparently need more dust than is observed, if we use $m_{\text{im}}(\text{dust}) = 0.005$. But, as pointed out above, $m_{\text{im}} = 0.005$ is not characteristic of any pure substance. In fact, the components of natural dust have highly contrasting imaginary indices and different size distributions. For New Mexico dust, Gillespie *et al.* (1978) did separate Mie calculations for the small-sized absorbing component (carbon) and the large-sized relatively transparent components and averaged the results. Compared to Mie quantities obtained using the “average” m_{im} , there were often large differences. In particular, the single-scattering albedo fell dramatically when the two components were treated separately. Mita and Isono (1980) also showed how, for the same weight-fractions of the two components, different size distributions of the absorptive component led to different “average” m_{im} values.

We saw that we could only match the Arctic snow

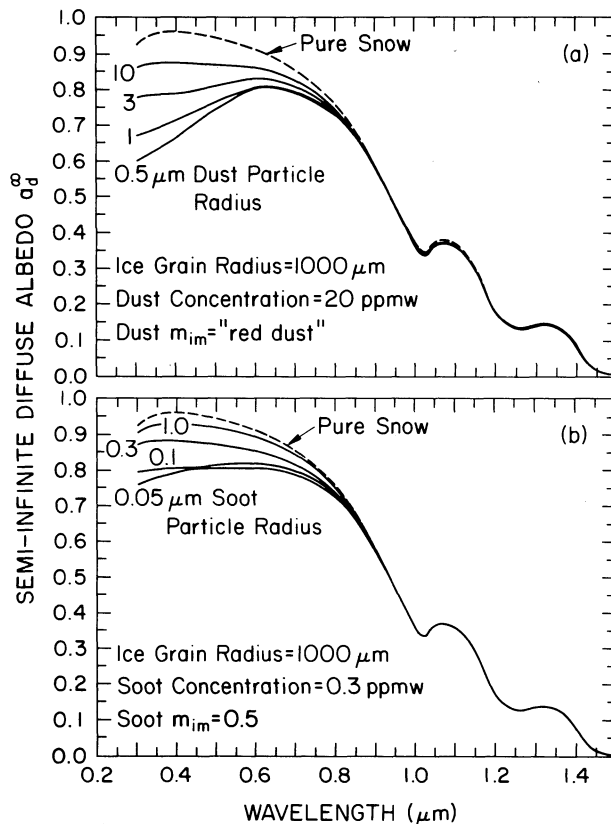


FIG. 4. Effect of (a) dust or (b) soot particle size on snow albedo a_d^{∞} .

albedo observations by the use of an m_{im} for dust that was fairly constant with wavelength (Fig. 6b). If the “average” m_{im} of dust is independent of wavelength, the absorptive component is most likely carbon. So we follow the example of Gillespie *et al.* and do Mie calculations for the carbon particles by themselves, ignoring the relatively transparent particles which are unimportant for snow albedo.

We assume soot is present in the snow as small particles of radius $0.1 \mu\text{m}$, density³ 2.05 g cm^{-3} , and refractive index $m = 1.8 - 0.5i$ (Twitty and Weisman, 1971). Fig. 3b shows the effect of soot on the single-scattering albedo of coarse-grained snow ($r = 1000 \mu\text{m}$). Comparison with Fig. 3a shows 1) the effect of 1 ppm of soot is as large as the effect of 100 ppm of dust; 2) soot affects $\bar{\omega}$ only at the short

³ (Note added in revision.) This density would be typical of a mixture of graphite and amorphous carbon. Together with the given values of r and m , it implies an absorption cross section at visible wavelengths of $3.7 \text{ m}^2 \text{ g}^{-1}$ (blue) to $5.7 \text{ m}^2 \text{ g}^{-1}$ (red). However, the individual $0.1 \mu\text{m}$ size soot particles may themselves contain gaseous inclusions, so that a more realistic density might be 1 g cm^{-3} (Rosen, personal communication), implying a visible absorption cross section of $7.4\text{--}11.5 \text{ m}^2 \text{ g}^{-1}$. If so, the reduction of snow albedo which we show for a given soot concentration should actually be attributed to half that concentration.

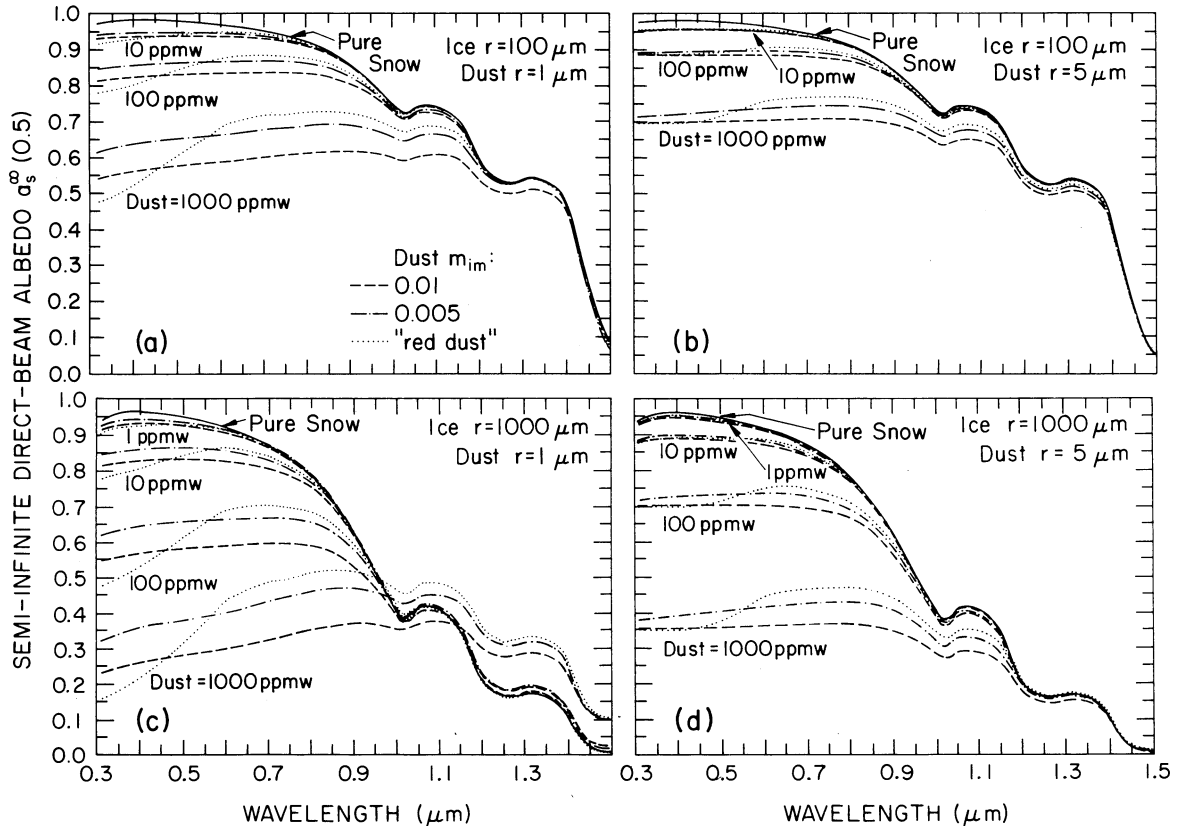


FIG. 5. Effect of snow and dust parameters on albedo a_s^z ($\mu_0 = 0.5$). The four frames are for different combinations of dust particle radius and snow grain radius. In each frame, results are shown for several dust concentrations. For each dust concentration, the albedo is plotted for three different $m_{im}(\lambda)$.

wavelengths (just as for dust); and 3) 1 ppm soot results in $(1 - \bar{\omega})$ rather constant with wavelength in the visible, whereas 100 ppm "red dust" gave a minimum at wavelength 0.6–0.7 μm .

The effect of soot particle radius on snow albedo is shown in Fig. 4b, for coarse-grained snow and a soot concentration of 0.3 ppmw. As for dust (Fig. 4a), the albedo drops as the soot particle size decreases. Twitty and Weinman (1971) suggested a model size distribution for soot particles which was based on observations of urban air by Peterson *et al.* (1969). When we used this distribution, we obtained the same spectral snow albedo as for the monodisperse $r = 0.1 \mu\text{m}$ case in Fig. 4b. Therefore, in all the calculations below which include soot we have used $r(\text{soot}) = 0.1 \mu\text{m}$. [Recently, Whitby (1979, Fig. 4) reported a bimodal size distribution, a "nuclei mode" at $r = 0.015 \mu\text{m}$ and an "accumulation mode" at $r = 0.1 \mu\text{m}$. As explained by Weiss *et al.* (1979, Fig. 2) and Bergstrom (1979, Fig. 1), this distribution should have the same absorption coefficient per unit mass as the monodisperse $r = 0.1 \mu\text{m}$ soot we are using.]

The effect of soot concentration on direct-beam ($\theta = 60^\circ$) snow albedo is shown in Fig. 7 for two different snow grain sizes. As with dust (Fig. 5), a par-

ticular concentration of soot is calculated to have much more effect on the albedo of old melting snow ($r = 1000 \mu\text{m}$) than on that of new snow ($r = 100 \mu\text{m}$).

The darkened snow is calculated to be essentially grey in the visible, in contrast to the strong peak in the red for red dust. A weight fraction of 10^{-7} for soot in snow ($r = 1000 \mu\text{m}$) is calculated to reduce the albedo at $\lambda = 0.4 \mu\text{m}$ by 7%. Even a weight fraction as low as 10^{-8} is calculated to reduce the albedo at this wavelength by 1%.

Fig. 6c shows that a soot concentration of 0.3–0.4 ppmw is required in our model to match the albedo observations of Grenfell and Maykut (1977). There are some discrepancies in exact shape between the two curves; they could be explained if the soot in the Arctic snow were found to have an m_{im} increasing slightly with wavelength instead of constant as we have assumed.

Measurements have not been published of concentrations of graphitic carbon in snow. If we accept Mullen *et al.*'s (1972) report of 1 ppm dust in snow at T-3, we are forced to hypothesize that 30–40% of the total dust is present as soot. This would not be unusual for an industrial city, but seems high for a remote area. However, the air in the high Arctic is often visibly polluted, most likely

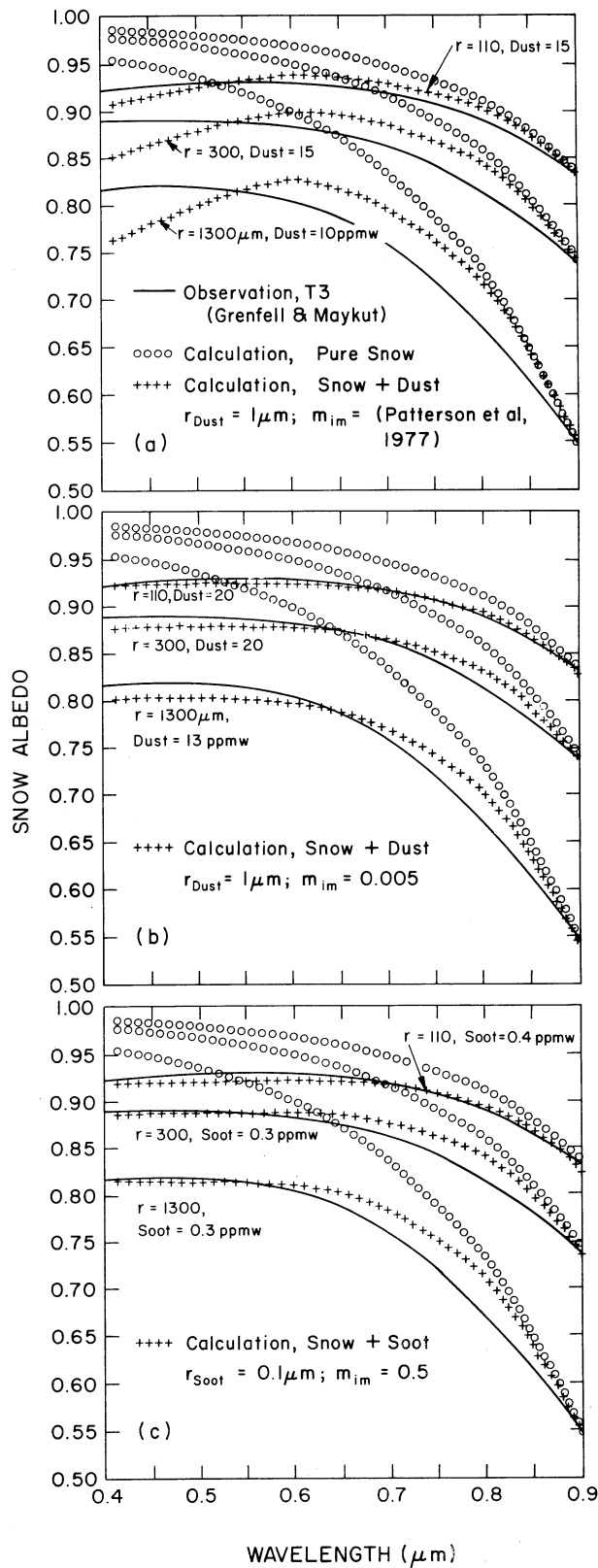


FIG. 6. Comparison of calculated snow albedo a_s^{∞} with observations. (a), (b) and (c) are identical except for the plus-sign curves which refer to different types of snow contamination.

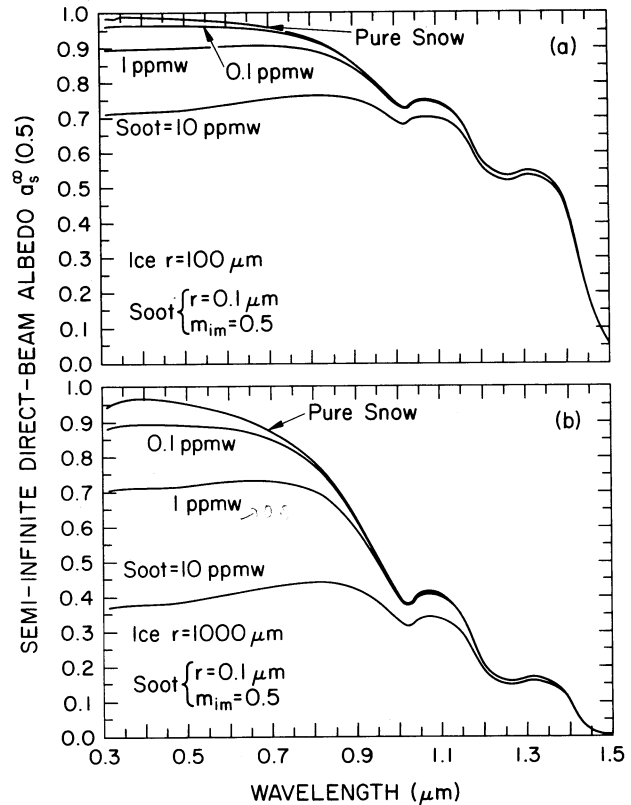


FIG. 7. Effect of soot concentration on albedo $a_s^{\infty}(\mu_0 = 0.5)$. (a) $r_{\text{ice}} = 100 \mu\text{m}$, (b) $r_{\text{ice}} = 1000 \mu\text{m}$.

from industrial sources in Europe (Rahn and McCaffrey, 1979; Rahn, personal communication). The concentrations of trace elements in the atmosphere at Barrow (Rahn and McCaffrey, 1979) are 4 to 10 times as high as in Greenland (Herron *et al.*, 1977) or in the Antarctic (Boutron and Lorius, 1979). The concentration of soot in air arriving at Barrow from the north ("the clean air sector") is as much as one-tenth of that in the air in New York City (Rosen, personal communication). Rahn (personal communication) estimates that soot would be present in Arctic snow at a level of 0.2 ppmw, within a factor of 2–3. This is based on 1) measured concentrations of noncrustal Mn in both snow and atmospheric aerosol at Barrow (Rahn and McCaffrey, 1979; Weiss *et al.*, 1978); 2) the measured fraction of soot in aerosol over Sweden (Brosset, 1978); and 3) the assumption that soot and Mn, both being in the submicron fraction, are removed from air into snow with the same efficiency.

In the absence of data on the soot content of snow, another speculation can be made from the estimates of Seiler and Crutzen (1980). They estimate the total worldwide production of graphitic carbon to be between 0.7 and $1.7 \times 10^{15} \text{ g year}^{-1}$, and that 20–30% of it becomes airborne. If we make the naive assumption that this is uniformly distributed over

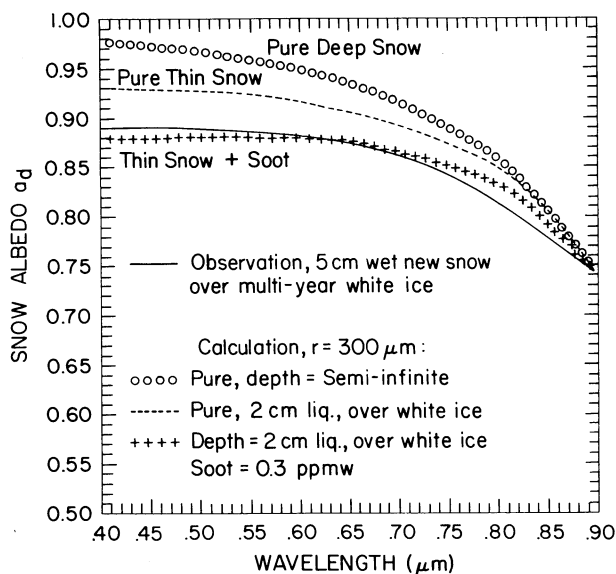


FIG. 8. Combined effect of finite depth and soot content on snow albedo a_d .

the earth's surface, the deposition rate would be 0.3 to 1.0 $\text{g m}^{-2} \text{year}^{-1}$. In the Arctic Ocean, where the mean annual precipitation is 13 $\text{g cm}^{-2} \text{year}^{-1}$, the carbon content would be 2–8 ppmw. This is 10–30 times as great as the amount of soot we think was present in the snow whose albedo was measured at T-3.

Even if the *general* level of soot in Arctic snow is insufficient to reduce the albedo, soot may still be the explanation of the low observed values at T-3. The measurements of Grenfell and Maykut (1977) were made within 500 m of the main camp on T-3, giving rise to the possibility of local pollution. The fuel which is burned for heating and electricity at Arctic and Antarctic camps typically releases 0.1–0.3% of its mass as soot particles (R. Charlson and J. Ogren, personal communication). Hanson (1980) noted that melt puddles on Arctic sea ice developed earliest in the camp areas, attributing this to soot contamination.

5. Combined effects of soot and finite depth on snow albedo

In Fig. 6 we used albedo calculations for a semi-infinite snowpack. However, one of the three snowpacks studied by Grenfell and Maykut (1977) was thin enough that we expect the underlying surface to influence the albedo. The middle solid line in Fig. 6 is for only 5 cm of wet new snow on top of multi-year white ice. We investigate the extent to which each of the two factors, finite depth and soot, can account for the reduction in albedo relative to that of pure deep snow. Both have the same qualitative effect, that of reducing the albedo only in the visible region.

Fig. 8 shows the wet new snow albedo measured by Grenfell and Maykut along with three model predictions. We assume the snow density was 0.4 g cm^{-2} , so that the snow depth was 2 cm liquid equivalent. The grain size is chosen as 300 μm to match the observed albedo at $\lambda = 0.9 \mu\text{m}$. The albedo of the underlying white ice we take as intermediate between curves *a* and *b* in Fig. 2 of Grenfell and Maykut (1977). This white ice has a maximum albedo of 0.84 at $\lambda = 0.4 \mu\text{m}$. The resulting albedo we calculate for the snow-ice system (without soot) is shown as the dashed line in Fig. 8. The albedo at $\lambda = 0.4 \mu\text{m}$ is reduced by 4.4%, relative to semi-infinite snow. If the underlying surface had been perfectly black, the albedo would have been reduced by 8% instead of 4.4%.

The finite-depth effect thus can only partially account for the observed albedo. In order to reduce the calculated albedo to the observed levels we require the addition of 0.3 ppmw soot (plus signs in Fig. 8). Thus, to explain observations we need the same amount of soot whether we take into account the finite depth (Fig. 8) or not (Fig. 6c). This is because light does not penetrate as deeply in the dirty snow as it does in pure snow. Two centimeter liquid equivalent of soot-containing snow is actually effectively semi-infinite in this case, whereas the same depth of pure snow is not.

This effect can also explain the paradox described in Section 5e of Part I. In their study of the effect of snow depth, Giddings and LaChapelle (1961, Fig. 2) found the snow albedo at $\lambda = 0.59 \mu\text{m}$ for grain size $\sim 250 \mu\text{m}$ and $\mu_0 = 1$ to be within 3% of the asymptotic limit for a depth of 2 cm ($\sim 8 \text{ mm}$ liquid equivalent). Fig. 13b in Part I shows that for pure snow about four times this depth would be required to reach within 3% of the semi-infinite albedo. The small 2 cm depth they observed corresponds to $\tau_0 \approx 120$ [Eq. (1) of Part I]. Our model for pure snow (Fig. 5b of Part I) would indicate that the semi-infinite limit when $(1 - \bar{\omega}) = 4 \times 10^{-3}$ (corresponding in Fig. 3 of Part I to $\lambda = 0.59 \mu\text{m}$ and $r = 250 \mu\text{m}$) is not attained until $\tau_0 \approx 300$, and that the asymptotic albedo is 95%, not the 75% measured by Giddings and LaChapelle. In order already at $\tau_0 = 120$ to reach an asymptotic albedo of 75%, $(1 - \bar{\omega})$ would be required to be an order of magnitude larger, around 10^{-3} (Fig. 5b, Part I). This can be achieved if the observed sample (from Alta, Utah) contained ~ 1 ppmw of soot. This amount of soot would explain the low asymptotic albedo of 75%, as well as the much smaller depth required to reach this asymptote.

6. Snow albedo at Antarctic stations

Measurements of impurities in falling snow and in Antarctic ice cores show Antarctic snow to be ex-

ceptionally clean. Typical values of total insoluble impurities (0.01–0.03 ppmw) are far too small to have any effect on snow albedo.

The spectral albedo measurements of Liljequist (1956), plotted in Fig. 17 of Part I, do indeed show very high values in tolerable agreement with our calculations for pure snow (up to $a_d = 97\%$ at $\lambda = 0.5 \mu\text{m}$). However, recent measurements by Kuhn and Siogas (1978) showed albedo values at the South Pole to be only $\sim 85\text{--}90\%$ through the visible spectrum. These measurements are shown in Fig. 1 and were discussed in the Introduction, where it was pointed out that for shorter wavelengths our calculated albedos (circles in Fig. 1) significantly exceeded the observed ones. In order to reduce the calculated visible albedo (while retaining agreement with observation in the near IR) we require the presence of 1.5 ppmw of soot.⁴ This is 50 to 100 times the concentration of *total* particulate matter observed in Antarctic ice cores, so this much soot cannot be naturally present in Antarctic snow. We think, however, that the particular snow sample examined here was contaminated by local pollution. The measurements were made ~ 1 km upwind from the South Pole station (Kuhn, personal communication). There is considerable soot released to the atmosphere here, both from aircraft exhaust in the summer and from furnaces and generators, especially in the winter. Also, in winter there are calm periods of strong surface temperature inversion during which the pollution dome extends in all directions, including the normal "upwind" direction. B. Parker and E. Zeller (personal communication), in the course of their chemical analyses of snow 2 km upwind from the South Pole, reported that all snow deposited since the establishment of the station during IGY (1957) contains visible filtrable carbon particles (radii $\geq 0.2 \mu\text{m}$) but that snow below the 1957 level does not contain those particles. Our opinion is that albedos measured farther from the station would be higher (for $\lambda < 0.9 \mu\text{m}$) than those shown by the solid line in Fig. 1, and that they would approximate the circles plotted for pure snow in Fig. 1.

Because of the very uniform surface conditions across the Antarctic plateau, energy-budget calculations (e.g., Weller, 1980) generally make the assumption that measurements at stations are representative of large areas of the interior. We would therefore like to warn that the existence of local pollution at the larger stations can make their local radiation conditions uncharacteristic of the surrounding region.

⁴ Kuhn (personal communication) calculates that his reported albedos should be adjusted upward by 4% (of their value) at all wavelengths due to the fact that the instrument box was in the field of view when the photometer head was facing downward. This means that we would require only 1 ppmw of soot to explain the measurement.

7. Summary

We have shown that the discrepancy between observations of visible snow albedo and calculations for pure snow (Fig. 17 of Part I) can be resolved if the snow whose albedo was measured was not pure. In order to match the observations of snow albedo at Station T-3 in the Arctic Ocean and at the South Pole Station, we require the presence of a grey impurity, i.e., one whose imaginary index of refraction varies little with wavelength. Graphitic carbon ("soot") has this property, and it is a normal component of the background atmospheric aerosol due to industrial sources as well as forest and brush fires. The snow at South Pole Station almost certainly suffers from local contamination and its albedo is unrepresentative of the rest of the Antarctic plateau where measured impurity concentrations are too low to affect the albedo.

Soot at T-3 in the Arctic Ocean, of which we require 0.3 ppmw to explain the albedo, may either be characteristic of the entire Arctic basin or derived from local (camp) pollution. This amount is not unrealistic if the soot which has been measured in Arctic air finds its way into the snow as well.

In middle latitudes the snow is closer to sources of dust and soot, but the snow accumulation rate is higher, so the concentration of impurities may not be larger until the snow begins to melt. The deposition rate of elemental carbon in Lake Michigan is now $30 \mu\text{g cm}^{-2} \text{ year}^{-1}$ (J. Herring, U.S.G.S., unpublished manuscript). It was only half this value prior to 1900. The morphology of the particles indicates about one-half charcoal and one-half industrial sources. Assuming an annual precipitation of 1 m (liquid equivalent), the snow near Lake Michigan would contain 0.3 ppmw soot, the same as we need to explain albedo observations in the Arctic Ocean (Fig. 6), where the annual precipitation is only one-tenth that of Lake Michigan.

It is difficult to analyze for graphitic carbon, particularly because it must be distinguished from organic carbon. It has not been looked for in any of the many snow-chemistry studies in Antarctica and Greenland. Due to the excellent experimental work of Rosen and Novakov (1977, 1978), however, it has now become possible to identify and measure the carbonaceous content of aerosols. In order to test the predictions of our model, it will be necessary to make simultaneous measurements of snow spectral albedo, snow grain size, soot concentration and soot size distribution.

The snow samples reviewed here were from Arctic and Antarctic locations, and they exhibited "grey" albedo in the visible. In snowfields closer to desert areas and remote from population centers, such as the ice caps of the Tibetan Plateau, the principal absorptive component of the dust may be

iron oxide instead of carbon. The snow would then exhibit a peak in the spectral albedo near $\lambda = 0.6 \mu\text{m}$ (Fig. 5), as has been seen by eye in Europe and New Zealand following dust storms in North Africa and Australia.

If the albedo of natural snow is being reduced by the presence of dust or soot, this could be an important climatic effect of tropospheric aerosols. Landsberg (1970) speculated that the climatic effects of aerosols in snow would be greater than their effects in the troposphere. Aerosols in the troposphere have competing effects on the radiation budget, in that they both absorb and reflect solar radiation, and emit infrared radiation. Carlson and Benjamin (1980) show that, for typical Saharan dust over the Atlantic, these effects roughly cancel each other for the top-of-atmosphere net flux. But when absorbing aerosols fall into snow, they have only one effect—that of reducing the shortwave albedo. The emissivity of snow in the infrared window region (8–12 μm) is very close to 1.0 (Figs. 8b and 11b of Part I) and the addition of parts-per-million amounts of dust does not change it.

In closing, we might note that *gross* amounts of carbon particles have in the past been suggested as effective melters of sea ice or modifiers of weather (Gray *et al.*, 1976). The present work indicates that such particles may have been having a climatic effect, albeit on a more subtle scale, over long periods of earth's history, which effect has been accentuated by man's industrial pollution.

Note added in proof. Grenfell *et al.* (1980) have recently collaborated to make simultaneous measurements of snow spectral albedo and soot content. Their measured grain sizes apparently are not the same as our effective spherical radii, so we deduce the effective optical grain size from the near-IR albedo measurements. It then appears that, in order to explain the visible albedos, we would need 2–5 times as much soot as was actually found in the snow. A factor of 2 difference in soot concentration can be explained by our use of graphite density instead of soot density (see footnote 3), but the remaining discrepancies remain to be investigated.

Acknowledgments. We thank Craig Bohren for first suggesting to us the importance of trace impurities in lowering snow albedo; Thomas Grenfell and Michael Kuhn for providing details of their experiments; and Robert Charlson, Peter MacKinnon, Kenneth Rahn, Hal Rosen, Lonnie Thompson and Ellen Mosley-Thompson for helpful discussion.

REFERENCES

- Becquerel, J., and J. Rossignol, 1929: Spectral absorption of light and heat by pure inorganic substances and miscellaneous materials (nonmetals). *International Critical Tables*, Vol. 5, McGraw-Hill, 268–271.
- Bergstrom, R. W., 1979: The effect of carbon particles on atmospheric radiation. *Carbonaceous Particles in the Atmosphere*, Lawrence Berkeley Laboratory, Publ. LBL-9037, 245–246.
- Boutron, C., and C. Lorius, 1979: Trace metals in Antarctic snows since 1914. *Nature*, **277**, 551–554.
- Brosset, C., 1978: Water-soluble sulphur compounds in aerosols. *Atmos. Environ.*, **12**, 25–38.
- Byers, H. R., 1936: Meteorological history of the brown snowfall of February 1936. *Mon. Wea. Rev.*, **64**, 86–87.
- Carlson, T. N., and S. G. Benjamin, 1980: Radiative heating rates for Saharan dust. *J. Atmos. Sci.*, **37**, 193–213.
- Dalzell, W. H., and A. F. Sarofim, 1969: Optical constants of soot and their application to heat-flux calculations. *J. Heat Transfer*, **91**, 100–104.
- Darby, D. A., L. H. Burckle and D. L. Clark, 1974: Airborne dust on the arctic pack ice, its composition and fallout rate. *Earth Planet. Sci. Lett.*, **24**, 166–172.
- Dirmhirn, I., 1960: Starke Absorptionsschichten auf den Schneeoberflächen der Alpengletscher. *Wetter und Leben*, **12**, 152–153.
- Dunne, T., and A. G. Price, 1975: Estimating daily net radiation over a snowpack. *Clim. Bull.*, McGill University, No. 18, 40–50.
- Elgmork, K., A. Hagen and A. Langeland, 1973: Polluted snow in southern Norway during the winters 1968–1971. *Environ. Pollut.*, **4**, 41–52.
- Falconer, R. E., and A. W. Hogan, 1971: Capture of aerosol particles by ice crystals. *Proc. Eastern Snow Conf.*, 1971, Fredericton, N.B., 1–8.
- Fischer, K., and G. Hänel, 1972: Bestimmung physikalischer Eigenschaften atmosphärischer aerosolteilchen über dem Atlantik. *Meteor. Forschungsergeb.*, Reihe B, **8**, 59–62.
- Foster, P. J., and C. R. Howarth, 1968: Optical constants of carbons and coals in the infrared. *Carbon*, **6**, 719–729.
- Franklin, Rosalind E., 1950: The structure of carbon. *J. Chim. Phys.*, **47**, 573–575.
- , 1951: The structure of graphitic carbons. *Acta Cryst.*, **4**, 253–261.
- Giddings, J. C., and E. R. LaChapelle, 1961: Diffusion theory applied to radiant energy distribution and albedo of snow. *J. Geophys. Res.*, **66**, 181–189.
- Gillespie, J. B., S. G. Jennings and J. D. Lindberg, 1978: Use of an average complex refractive index in atmospheric propagation calculations. *Appl. Opt.*, **17**, 989–991.
- Glazovskaya, M. A., 1954: Eolian deposits on Tien Shan glaciers (in Russian). *Priroda*, **43**, 90–92.
- Gray, W. M., W. M. Frank, M. L. Corrin and C. A. Stokes, 1976: Weather modification by carbon dust absorption of solar energy. *J. Appl. Meteor.*, **15**, 355–386.
- Greenaway, D. L., G. Harbeke, F. Bassani and E. Tosatti, 1969: Anisotropy of the optical constants and the band structure of graphite. *Phys. Rev.*, **178**, 1340–1348.
- Grenfell, T. C., and G. A. Maykut, 1977: The optical properties of snow and ice in the Arctic basin. *J. Glaciol.*, **18**, 445–463.
- , D. K. Perovich and J. A. Ogren, 1980: Spectral albedos of an Alpine snowpack. *Cold Regions Sci. Tech.* (in press).
- Haerberli, W., 1977: Sahara dust in the Alps—A short review. *Z. Gletscher. Glazialgeol.*, **13**, 206–208.
- Hamilton, W. L., and C. C. Langway, Jr., 1967: A correlation of microparticle concentrations with oxygen isotope ratios in 700-year old Greenland ice. *Earth. Plan. Sci. Lett.*, **3**, 363–366.
- Hammer, C. U., 1977: Dating of Greenland ice cores by microparticle concentration analyses. *Isotopes and Impurities in Snow and Ice*, IAHS Publ. No. 118, 297–301.
- Hanson, A. M., 1980: The snow cover of sea ice during the Arctic ice dynamics joint experiment, 1975 to 1976. *Arctic Alpine Res.*, **12**, 215–226.
- Hanson, K. J., 1960: Radiation measurement on the Antarctic

- snowfield, a preliminary report. *J. Geophys. Res.*, **65**, 935–946.
- Herron, M. M., C. C. Langway, Jr., H. V. Weiss and J. H. Cragin, 1977: Atmospheric trace metals and sulfate in the Greenland ice sheet. *Geochim. Cosmochim. Acta*, **41**, 915–920.
- Higuchi, K., and A. Nagoshi, 1977: Effect of particulate matter in surface snow layers on the albedo of perennial snow patches. *Isotopes and Impurities in Snow and Ice*, IAHS Publ. No. 118, 95–97.
- Khromov, S., 1931: Yellow snow (in Russian). *Mirovendenie*, **20**, 106–107.
- Koerner, R. M., 1977: Distribution of microparticles in a 299 m core through the Devon Island ice cap, Northwest Territories, Canada. *Isotopes and Impurities in Snow and Ice*, IAHS Publ. No. 118, 371–376.
- Kohno, S., and N. Maeno, 1979: Migration of solid particles in melting snow. *Low Temp. Sci.*, **A38**, 81–92.
- Kuhn, M., and L. Siogas, 1978: Spectroscopic studies at McMurdo, South Pole and Siple Stations during the austral summer 1977–78. *Antarctic J. U.S.*, **13**, 178–179.
- Kumai, M., 1976: Identification of nuclei and concentrations of chemical species in snow crystals sampled at the South Pole. *J. Atmos. Sci.*, **33**, 833–841.
- , 1977: Electron microscope analysis of aerosols in snow and deep ice cores from Greenland. *Isotopes and Impurities in Snow and Ice*. IAHS Publ. No. 118, 341–350.
- Landsberg, H. E., 1970: Man-made climatic changes. *Science*, **170**, 1265–1274.
- Langway, C. C., Jr., G. A. Klouda, M. M. Herron and J. H. Cragin, 1977: Seasonal variations of chemical constituents in annual layers of Greenland deep ice deposits. *Isotopes and Impurities in Snow and Ice*, IAHS Publ. No. 118, 302–306.
- Liljequist, G. H., 1956: Energy exchange of an Antarctic snowfield. Short-wave radiation (Maudheim, 71°03'S, 10°56'W). *Norwegian-British-Swedish Antarctic Expedition, 1949–52, Scientific Results*, Vol. 2, Part 1A, Norsk Polarinstittut, 107 pp.
- Lindberg, J. D., 1975: The composition and optical absorption coefficient of atmospheric particulate matter. *Opt. Quant. Electron.*, **7**(Review), 131–139.
- Magono, C., T. Endoh, F. Ueno, S. Kubota and M. Itasaka, 1979: Direct observations of aerosols attached to falling snow crystals. *Tellus*, **31**, 102–114.
- Marshall, P., and E. Kidson, 1929: The dust-storm of October 1928. *N.Z. J. Sci. Tech.*, **10**, 291–299.
- McCartney, J. T., J. B. Yasinsky and S. Ergun, 1965: Optical constants of coals by reflectance measurements in the ultraviolet and visible spectrum. *Fuel*, **44**, 349–354.
- Mita, A., and K. Isono, 1980: Effective complex refractive index of atmospheric aerosols containing absorbing substances. *J. Meteor. Soc. Japan*, **58**, 69–80.
- Mullen, R. E., D. A. Darby and D. L. Clark, 1972: Significance of atmospheric dust and ice rafting for Arctic Ocean sediment. *Geol. Soc. Amer. Bull.*, **83**, 205–212.
- Murozumi, M., T. J. Chow and C. Patterson, 1969: Chemical concentrations of pollutant lead aerosols, terrestrial dusts and sea salts in Greenland and Antarctic snow strata. *Geochim. Cosmochim. Acta*, **33**, 1247–1294.
- Oeschger, H., U. Schotterer, B. Stauffer, W. Haeberli and H. Röthlisberger, 1977: First results from alpine core drilling projects. *Z. Gletscher. Glazialgeol.*, **13**, 193–204.
- Patterson, E. M., and D. A. Gillette, 1977: Commonalities in measured size distributions for aerosols having a soil-derived component. *J. Geophys. Res.*, **82**, 2074–2082.
- , D. A. Gillette and B. H. Stockton, 1977: Complex index of refraction between 300 and 700 nm for Saharan aerosols. *J. Geophys. Res.*, **82**, 3153–3160.
- Peterson, C. M., H. J. Paulus and G. H. Foley, 1969: The number-size distribution of atmospheric particles during temperature inversions. *J. Air Pollut. Control Assoc.*, **19**, 795–801.
- Pollack, J. B., O. B. Toon and B. N. Khare, 1973: Optical properties of some terrestrial rocks and glasses. *Icarus*, **19**, 372–389.
- Post, A., and E. R. LaChapelle, 1971: *Glacier Ice*. University of Washington Press, 110 pp.
- Prospero, J. M., 1979: Mineral and sea salt aerosol concentrations in various ocean regions. *J. Geophys. Res.*, **84**, 725–731.
- Pruppacher, H. R., and J. D. Klett, 1978: *Microphysics of Clouds and Precipitation*. Reidel, 714 pp.
- Rahn, K. A., and R. J. McCaffrey, 1979: Compositional differences between Arctic aerosol and snow. *Nature*, **280**, 479–480.
- Robinson, W. O., 1936: Composition and origin of dust in the fall of brown snow, New Hampshire and Vermont, February 24, 1936. *Mon. Wea. Rev.*, **64**, 86.
- Rosen, H., and T. Novakov, 1977: Raman scattering and the characterization of atmospheric aerosol particles. *Nature*, **266**, 708–710.
- , and —, 1978: Identification of primary particulate carbon and sulfate species by Raman spectroscopy. *Atmos. Environ.*, **12**, 923–927.
- , A. D. A. Hansen, L. Gundel and T. Novakov, 1978: Identification of the optically absorbing component in urban aerosols. *Appl. Opt.*, **17**, 3859–3861.
- Seiler, W., and P. J. Crutzen, 1980: Estimates of gross and net fluxes of carbon between the biosphere and the atmosphere from biomass burning. *Climatic Change*, **2**, 207–247.
- Stephenson, P. J., 1967: Some considerations of snow metamorphism in the Antarctic ice sheet in the light of ice crystal studies. *Physics of Snow and Ice, Proceedings of the International Conference on Low Temperature Sciences*, H. Ōura, Ed., 14–19 August 1966, Sapporo, Japan, Bunyeido Printing Company, 725–740.
- Thompson, L. G., 1977: Variations in microparticle concentration, size distribution and elemental composition found in Camp Century, Greenland, and Byrd Station, Antarctica, deep ice cores. *Isotopes and Impurities in Snow and Ice*, IAHS Publ. No. 118, 351–364.
- , S. Hastenrath and B. Morales-Arnao, 1979: Climatic ice core records from the tropical Quelccaya Ice Cap. *Science*, **203**, 1240–1243.
- Toon, O. B., J. B. Pollack and B. N. Khare, 1976: The optical constants of several atmospheric aerosol species: Ammonium sulfate, aluminum oxide and sodium chloride. *J. Geophys. Res.*, **81**, 5733–5748.
- Twitty, J. T., and J. A. Weinman, 1971: Radiative properties of carbonaceous aerosols. *J. Appl. Meteor.*, **10**, 725–731.
- Weiss, H. V., M. M. Herron and C. C. Langway, Jr., 1978: Natural enrichment of elements in snow. *Nature*, **274**, 352–353.
- Weiss, R. E., A. P. Waggoner, R. Charlson, D. L. Thorsell, J. S. Hall and L. A. Riley, 1979: Studies of the optical physical and chemical properties of light absorbing aerosols. *Carbonaceous Particles in the Atmosphere*, Lawrence Berkeley Laboratory, Publ. LBL-9037, 257–262.
- Weller, G. E., 1980: Spatial and temporal variations in the south polar surface energy balance. *Mon. Wea. Rev.*, **108**, 2006–2014.
- Whitby, K. T., 1979: Size distribution and physical properties of combustion aerosols. *Carbonaceous Particles in the Atmosphere*, Lawrence Berkeley Laboratory, Publ. LBL-9037, 201–208.
- Windom, H. L., 1969: Atmospheric dust records in permanent snowfields: Implications to marine sedimentation. *Geol. Soc. Amer. Bull.*, **80**, 761–782.
- Wiscombe, W. J., and S. G. Warren, 1980: A model for the spectral albedo of snow. I. Pure snow. *J. Atmos. Sci.*, **37**, 2712–2733.